LANDSLIDE MAPPING BY TEXTURAL ANALYSIS OF ATM DATA*

Javier Hervás and Paul L. Rosin

European Commission
Joint Research Centre
Institute for Remote Sensing Applications
21020 Ispra (Va), Italy

ABSTRACT

In this paper we evaluate two statistical approaches to semi-automated texture enhancement and discrimination for landslide mapping in semi-arid, sedimentary terrain from Daedalus ATM data. A supervised texture discrimination technique is applied, based on calculating similarity between a reference texture spectrum obtained from training samples and spectra from moving image windows. The results are compared with those from interpreting a set of popular texture measures from the literature, derived from grey level co-occurrence matrix statistics. In this comparison, interpretation is facilitated by statistical selection of the best combination of three measures using a sequential forward search algorithm. It is concluded that the texture spectrum based discrimination technique proves superior to using pre-defined sets of texture measures, since it is able to highlight areas on imagery which are often associated with disrupted, displaced land masses.

1.0 INTRODUCTION

Landslides may produce complex slope surface patterns not readily distinguished visually on remotely sensed data. These spatial features are largely dependent on the geotechnical properties of the ground, slope gradient and land cover type, and are often expressed as local topographic variations such as scarps and hummocky slope surfaces. These landforms acquire a dominant role over other possible indicators when mapping natural slope instability on semi-arid terrain.

In the context of remotely sensed digital imagery, approaches to landslide mapping are commonly based on a combination of textural and spectral enhancements (Eyers *et al*, 1995). Here, textural enhancement is frequently accomplished by spatial filtering followed by contrast enhancement. This approach has proved useful, and can be easily implemented. However, the algorithm parameters have usually to be carefully tuned up to the study area properties. Furthermore, the products thus obtained often require a great deal of time for interpretation.

Automatic texture analysis has been successful in discriminating regular patterns in many machine vision applications. However, a more serious challenge is posed when it is applied to remotely sensed

Presented at the Eleventh Thematic Conference and Workshops on Applied Geologic Remote Sensing, Las Vegas, Nevada, 27-29 February 1996

data because of the irregular and less distinctive patterns usually occurring in nature. In this paper we evaluate two statistical approaches to texture enhancement and discrimination for semi-automated mapping hummocky slid terrain from Daedalus ATM data over a semi-arid moderate-relief area in SE Spain. The first approach regards the use of texture measures (Haralick *et al*, 1973; Haralick 1979; Baraldi and Parmiggiani, 1995). These measures contain information about the spatial distribution of local grey-level variations within a band. In the second approach, image texture is defined in terms of frequency distribution of local intensity variation by means of its "texture spectrum" (Wang and He, 1990). From this, a supervised texture discrimination technique is applied to identify areas with possible slides. Statistical and empirical methods to select the best texture measures and algorithm parameters, as well as the introduction of subtle variations to the original algorithms are also discussed.

2.0 STUDY AREA

The study area is located in Los Vélez district, at the boundary between Andalucia and Murcia in south-east Spain. This site includes complex terrain patterns in terms of both landforms and land use, which are very representative of the various natural conditions found in extensive areas of south and south-east Spain.

Geologically, most of the area belongs to the Penibetic-Subbetic Zone of the Betic Cordillera, the southernmost alpine range in Europe. This Zone forms a large and complex east-north-east trending nappe comprising a Mesozoic-Lower Tertiary lithological sequence (IGME, 1977 and 1979). Major parent lithologies in the area include Jurassic limestone and dolomite, Upper Cretaceous flyschoid sequences of marls and marly limestone, and Lower Miocene clays and marls. Limestone and dolomite form ridges or hills with steep slopes and cliffs. At their feet, clay, marls and marly limestone are partly overlaid by conglomerate colluvium and glacis of Quaternary age. They form overall gentle slopes which are densely cut off by highly-erosive, narrow gullies, most of them with ephemeral streams. Each of all major lithological units in the area make part of different structural units, where the Jurassic limestone and dolomite groups overthrust all the others. The Penibetic-Subbetic nappe overthrusts the Silurian-Eocene sandstone, phyllite and dolomite materials of the Malaguide Complex at the south end of the study area. A general geotechnical description of the various lithological groups can be found in MOP (1971).

The Los Vélez district is a Mediterranean semi-arid area with average annual rainfall of 400 mm. This is usually concentrated during short time periods in autumn and spring. Vegetation is in general scarce. It mainly consists of herbs and shrubs such as thyme, rosmarinus and stipa, especially on cemented colluvium. Stony soil and rock exposures clearly show up in between the scarce vegetation, the latter mainly on limestone hill slopes. There are, however, numerous patches of haleppo pine which have been grown on small terraces over the various lithologies in the area during the last decades to fight erosion and sliding, as well as scattered pine trees and bushes on colluvial soils. Almond trees, olive trees, orchards and some cereals are grown on terraces and small low slope zones over the Tertiary and Quaternary sediments in the centre of the area.

Landslides occur mainly on dark green and greenish-brown clays and marls of Lower Miocene age, which often includes gypsum crystals and some sandstone layers locally. They appear at the foot

of the limestone and dolomite ridges and hills, and at gully sides. Often these formations are capped by cemented conglomerate colluvium which slides together with the underlying materials. Using the nomenclature from UNESCO (1993) and IAEG (1990), the slope movements correspond to rotational slides, both single and multiple, and composite rotational-slides rock-falls. Scarps are only apparent in some slides. The surface dimensions of the displaced masses range from 100 to 800 metres either along or across the major movement direction. Most slides show a characteristic hummocky surface made up of an irregular succession of depletion and accumulation zones.

Although we did not find records of landslide activity, it was inferred from old aerial photography, field checking and local farmers information, that sliding still occurs on gully sides after heavy rainfall periods. Largest landslides were probably triggered in older times by earthquakes most likely coupled with groundwater pressure at the thrust boundary between limestone and clay. Although they appear mostly inactive, some readjustments still occur occasionally after heavy rain. Therefore they still represent a threat to property and infrastructure while they contribute to soil erosion. Large composite fossil slides are also present in the area. They show calcareous mounts embedded in the Miocene clays and are not easily recognised in the field. They have not been considered in this work. Slides of the types studied in Los Vélez district are commonplace in the Cretaceous and Miocene clays and marls of the Subbetic and structurally associated zones spreading across Andalucia and Murcia regions (Hervás and Prieto, 1981).

3.0 DIGITAL DATA

For this study Daedalus AADS 1268 Airborne Thematic Mapper (ATM) data were used. The ATM sensor acquires imagery in 11 spectral bands from the visible to the thermal infrared. A number of swathes were flown by INTA of Torrejón, Spain, on 26th April 1994 just before noon. A 6051×883 pixel swathe with a nominal pixel size of 3.5 metre at nadir was then selected. This covers an area approximately 16 km long by 2.5 km wide. A ground survey was undertaken simultaneously with the ATM flights.

The wide field of view of the ATM causes some panoramic distortion across the swath, which was corrected during pre-processing, as were the roll effects. No further geometric correction was attempted since it was not regarded relevant for this kind of investigation. Possible across-track differential sun illumination effects were reduced to a minimum by flying swathes at a time when high sun elevation angle is relatively high, while its azimuth is far from the across-track scanning direction. This effect was not immediately apparent in the data, therefore no attempt was made to correct for it.

4.0 METHODOLOGY

4.1 TEXTURE MEASURE APPROACH

Statistical texture measures are concerned with the spatial distribution and spatial dependence among the image pixel values in a local area. These measures are extracted from grey-level co-occurrence matrices (Haralick *et al*, 1973; Haralick, 1979).

In this work we evaluate the usefulness for landslide mapping of 14 textural measures selected from among those reported successful in the literature for various remote sensing applications. Some of these have been originally proposed by Haralick *et al* (1973), such as Angular Second Moment, Contrast, Correlation, Variance, Inverse Difference Moment, Sum Average, Sum Variance, Sum Entropy, Entropy, Difference Variance, Difference Entropy and Second Measure of Correlation. Others such as Recursivity and Inverse Recursivity were proposed by Baraldi and Parmiggiani (1995).

Since the most suitable features and parameters for our investigation were not known a priori some means is required for their determination. However, exhaustively testing all possibilities is prohibitively expensive. For instance, if the 14 texture features above were derived for each of the 11 ATM bands, and each feature computed for the 4 co-occurrence matrix orientations, for 3 matrix sizes (w), 3 inter-sample spacing values (d), and 3 different pixel increments (i) for moving the matrix both in the row and column directions, then 16,632 texture images would have to be generated. A substantial reduction of this large data set therefore becomes necessary.

From both visual inspection and preliminary processing of the ATM data, it was decided to use only band 11 (8.5 μm - 13.5 μm) in this experiment. This band captures thermally emitted energy with dominant effect of surface temperature. Daytime thermal imagery in the area is sensitive to topography and therefore to geomorphology while is less sensitive to land use and lithological variations. Basic spectral enhancement techniques for characterising possible variations of vegetation patterns, soil moisture or lithologies between the slid and surrounding non-slid areas using other bands generally proved inefficient. This was mainly due to the steady drought conditions in the area, the single time acquisition and the lack of significant lithological changes around the displaced mass. Alternatively, a median filtered band 11 image could be used as it removes disturbing "scene noise" like isolated trees and bushes, which are easily picked out on high spatial resolution imagery, while preserving geomorphologic information such as hummocky terrain and arcuate scarps.

4.1.1 Best Parameter and Measure Selection

In order to further reduce the large number of such possible combinations, we start making a selection of the best parameters for a random single measure and then select the best measure with those parameters, out of the 14 considered. This can be done, for instance, for Variance, which is a generally middle-ranked measure in terms of usefulness for texture mapping. For any set of texture images thus created, we select the best combination of n images from N images by using the sequential forward search (SFS) algorithm (Devijver and Kittler, 1982). To avoid the combinatorial explosion incurred when considering all possible texture image combinations, namely $\binom{N}{n}$, SFS provides a more practical, but suboptimal, approach. Given some criterion function which is to be minimised say, the best single image is first selected. Then all combinations of image pairs including the best single image are evaluated, and the best pair is retained. The process is repeated, each time adding a new image to the previous set until n images are obtained.

For a region R (which may be composed of non-adjacent subregions) that we wish to discriminate with respect to the remainder of the image we calculate its mean $\mathbf{m}$ and covariance matrix $\mathbf{C}$. Then

we use the Mahalanobis distance D as the discrimination function, comparing the region parameters with the remainder of the image:

$$D^2 = \sum_{(x,y)\notin R} \left[\left(\mathbf{I}_{x,y} - \mathbf{m} \right) \mathbf{C}^{-1} \left(\mathbf{I}_{x,y} - \mathbf{m} \right)^{\mathrm{T}} \right]$$

The advantages of the Mahalanobis distance are that incorporating the covariance matrix enables it to take any correlation between different images into account, and to penalise texture images which have a high variance in the region of interest.

In our experiments we iteratively applied the SFS algorithm to a large subset of the possible parameters available with the co-occurrence matrix method. The best *i* value out of 1, 4 and 8 is first selected from the texture image of the Variance measure for ATM band 11, with d = 1 pixel and w = 8 pixels. An averaged value for the four matrix orientations is used. Texture images with *w* values of 8, 16 and 32 are then tested by the algorithm for the *i* value previously selected, and the best *w* is then extracted. The process is repeated for d values of 1, 2 and 4. The best values thus selected for the Variance parameters are i = 1, w = 16 and d = 1. These values are then used in the selection of the 3 best ranked texture features, resulting in Entropy, Recursivity and Second Measure of Correlation, respectively.

4.2 TEXTURE SPECTRUM APPROACH

The texture spectrum approach (Wang and He, 1990) first considers texture units (E_i) by analysing each 3×3 window. The central value V_c is compared to its 8 nearest neighbours V_i or, alternately, to longer distance neighbours, which are assigned one of three values E_i determined by

$$E_i = \begin{cases} 0 & \text{if } V_i < V_c \\ 1 & \text{if } V_i = V_c \\ 2 & \text{if } V_i > V_c \end{cases}$$

From E_i the texture unit number is generated by

$$N_{TU} = \sum_{i=1}^{8} 3^{i-1} E_i; \quad N_{TU} \in \{0,1,2,\ldots,6560\}$$

For each $w \times w$ window in the image a texture spectrum is generated by histogramming the texture unit numbers that occur within the window (Figure 1). Similarity between textures can now be compared by taking the absolute differences between their texture spectra. Thus, for two texture spectra A_i and B_i where $i \in \{0,1,2,\ldots,6560\}$, their similarity is

$$S = \sum_{i=0}^{6560} \left| A_i - B_i \right|$$

For our purposes we generate the training texture spectrum T_i from the area(s) of interest (of arbitrary size and shape), corresponding to known landslide(s), over ATM band 11. This spectrum is normalised to a frequency by dividing each element of the histogram by the area of the region.

Supervised texture discrimination is then carried out by assigning to each pixel in the image the similarity S calculated from the difference between T_i and the image texture spectrum $W_i(x,y)$ calculated in the $w \times w$ window centred at (x,y)

$$S_{x,y} = \sum_{i=0}^{6560} \left| T_i - W_i(x,y) \right|$$

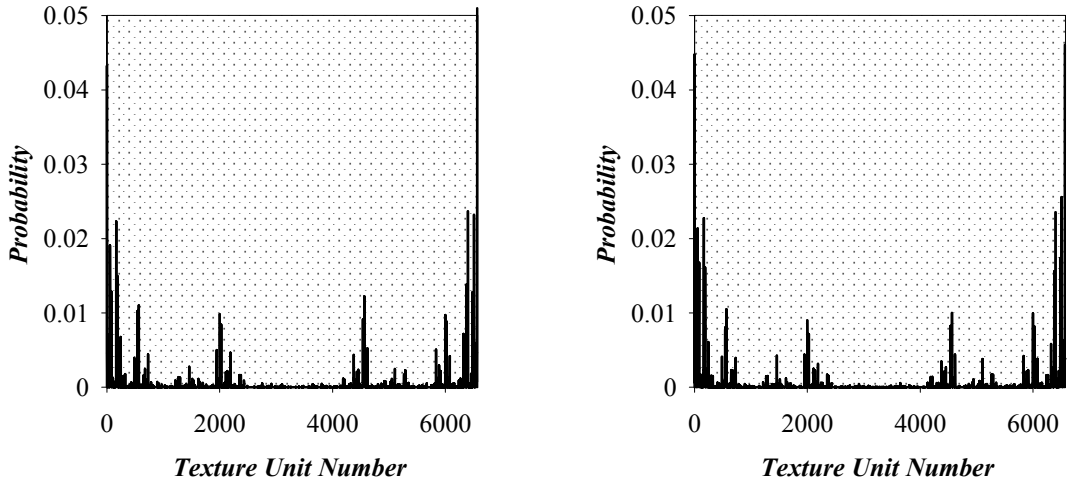

Figure 1. (a) Training Texture Spectrum T_i. (b) Image Texture Spectrum W_i

Since in most cases pixels do not have precisely identical values to their neighbours a more efficient version is to generate texture units using only two values

$$E_i = \begin{cases} 0 & \text{if } V_i < V_c \\ 1 & \text{if } V_i > V_c \end{cases}$$

while in the situation that $V_i = V_c$ either the texture unit number can be discarded, or E_i can be randomly assigned either 0 or 1, and the resulting texture unit number retained. We take the latter approach. Using 2 rather than 3 values means that much shorter texture spectra are generated (containing 256 rather than 6561 values), providing a substantial improvement in efficiency for only a slight degradation in quality. In either version image pixels are subsequently normalised to [0, 255].

5.0 RESULTS

The 3 statistically-selected texture measures are able to discriminate between rough and smooth surfaces. However, in the study area the distinction between known landslides, small gullies and cultivation terraces is generally not possible in any of these texture images. The Entropy image (Figure 2c), as first-ranked by the SFS algorithm, does not appear in general superior to Recursivity and

Second Measure of Correlation for mapping possible sliding. Nonetheless, these measures are proved superior to other randomly-selected measures. In a false colour composite of these three texture images discrimination of gullies and slides is improved with respect to single measures, but this is not yet a very useful product to differentiate slides by its own. Furthermore, hummocky slid terrain cannot be distinguished from closed pine trees stands. These texture measures can be useful for landslide mapping only as a preliminary image segmentation technique.

The texture spectrum method outputs an image where very low pixel value areas are often associated with landslides and disrupted terrain. From testing a few variations of the possible texture spectrum algorithm parameters, it was found that selecting a minimum of 2 training sites, a moving window ($w \times w$) of 81×81 pixels and a pixel increment of 4 for moving the window both in the row and column directions, resulted in a satisfactory image to map potential and existing slide areas. In this density-sliced image (Figure 2b), forest stands and regularly spaced trees crops are clearly discriminated from known displaced land masses. Incipient bad-lands and some area with irregular limestone exposures appear undifferentiated from landslides. The former may hinder detecting existing instability on gully sides.

In our data, larger algorithm window sizes and pixel increments tend to smooth the image, making the site discrimination more difficult. Smaller windows and pixel increments can result in relatively noisy images, enhancing non-relevant spatial frequency content.

6.0 CONCLUSIONS

Two semi-automated, statistical texture approaches for mapping landslide geomorphologic features in semi-arid terrain have been analysed using single acquisition, high spatial resolution optical data.

Some predefined texture measures can be useful in this type of research for preliminary image segmentation. In addition, the ability of some of the local statistics properties as edge enhancers becomes apparent. Selected measures using a discriminant function prove to be a more objective approach, and can thus be used irrespective of the study area. This approach can be fairly automated, although it requires substantial computer processing. Texture spectrum based discrimination proves a more suitable and cost-effective method, since it is able to highlight areas on imagery often associated to sliding, and suspect areas where detailed site investigations are needed. However, in both approaches landslides are not easily differentiated from dense erosion patterns. Investigations are continuing to test the methodology to lower spatial resolution images and further tune the algorithm parameters.

7.0 ACKNOWLEDGEMENTS

The authors are most grateful to M.J. Gutiérrez de la Cámara, Alix Fernández-Renau and J.A. Gómez of INTA, Torrejón, Spain, for the supply and pre-processing of the Daedalus ATM data used in this study. Thanks are due to C. León and M. Rodríguez of the Roads Directorate, MOPTMA, Madrid, for their help in landslide field checking and aerial photointerpretation. Thanks are also due to our colleague S. Sommer for advice in the planning of the airborne campaign.

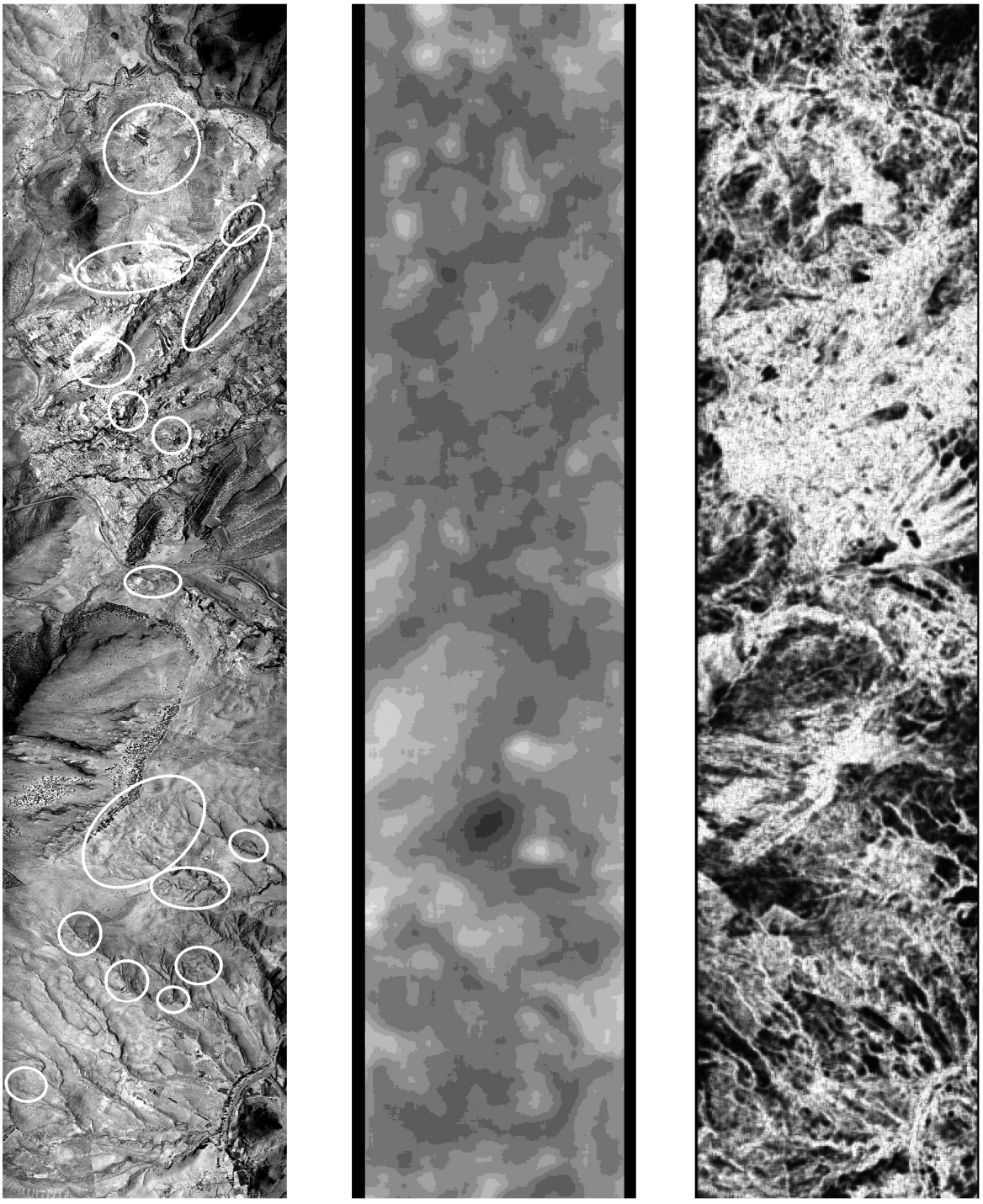

(a) (b) (c)

Figure 2. (a) ATM Band 11. Known landslide sites are circled.
(b) Texture Spectrun Based Segmentation. (c) Entropy Image

8.0 REFERENCES

Baraldi, A. and F. Parmiggiani, 1995. "An investigation of the textural characteristics associated with grey level co-occurrence matrix statistical parameters", *IEEE Trans. Geosci. Remote Sensing*, Vol. 33, 2, pp. 293-304.

Devijver, P.A. and J. Kittler, 1982. *Pattern Recognition. A Statistical Approach*, Prentice-Hall, Englewood Cliffs, New Jersey, USA.

Eyers, R., J. Moore, J. Hervás and J.G. Liu, 1995. "Landslide mapping using digital imagery: a case history from south east Spain", *Proc. 31st Annual Conf.: Geohazards and Engineering Geology*, Coventry, UK, 10-14 September 1995. The Geological Society, pp. 379-388.

Haralick, R.M., K. Shanmugan and I. Dinstein, 1973. "Textural features for image classification", *IEEE. Trans. Syst., Man, Cybern*., Vol. SMC-3, 6, pp. 610-621.

Haralick, R.M., 1979. Statistical and structural approaches to texture, *Proc. IEEE*, Vol. 67, 5, pp. 786-804.

Hervás, J. and C. Prieto, 1981. "Estudio de movimientos del terreno en la provincia de Granada", *Ministerio de Obras Públicas, Transportes y Medio Ambiente, Dirección General de Carreteras*, Madrid, Spain. Internal Report, 3 Vol.

IAEG Commission on Landslides, 1990. "Suggested nomenclature for landslides". *Bull. International Association of Engineering Geology*, No. 41, pp 13-16.

IGME, 1977. "Mapa Geológico de España: Sheet 952 Vélez-Blanco, scale 1:50000". *ITGE*, Madrid.

IGME, 1979. "Mapa Geológico de España: Sheet 974 Vélez-Rubio, scale 1:50000". *ITGE*, Madrid.

MOP, 1971. "Estudio previo de terrenos, autopista del Mediterráneo, tramo: Lorca-Vélez Rubio", *Ministerio de Obras Públicas, Transportes y Medio Ambiente, Dirección General de Carreteras*, Madrid, Spain. p. 119.

UNESCO Working Party on World Landslide Inventory, 1993. "A suggested method for describing the activity of a landslide", *Bull. International Association of Engineering Geology*, No. 43, pp. 53-57.

Wang, L. and D.C. He, 1990. "A new statistical approach for texture analysis", *Photogram. Eng. Remote Sensing*, Vol. 56, 1, pp. 61-66.